J. theor. Biol. (2000) **206,** 91–107
doi:10.1006/jtbi.2000.2107, available online at http://www.idealibrary.com on IDEAL®

Transpiration and Assimilation of Early Devonian Land Plants with Axially Symmetric Telomes—Simulations on the Tissue Level

W. Konrad*, A. Roth-Nebelsick*†, H. Kerp‡ and H. Hass‡

**Institut und Museum für Geologie und Paläontologie, Sigwartstr.* 10, *D*-72076 *Tübingen, Germany and*
‡*Abteilung Paläobotanik, Westfälische Wilhelms-Universität Münster, Hindenburgplatz* 57–59, *D*-48143 *Münster, Germany*

(*Received on* 9 *December* 1999, *Accepted in revised form on* 12 *May* 2000)

Early terrestrial ancestors of the land flora are characterized by a simple, axially symmetric habit and evolved in an atmosphere with much higher CO_2 concentrations than today. In order to gain information about the ecophysiological interrelationships of these plants, a model dealing with their gaseous exchange, which is basic to transpiration and photosynthesis, is introduced. The model is based on gas diffusion inside a porous medium and on a well-established photosynthesis model and allows for the simulation of the local gas fluxes through the various tissue layers of a plant axis. Necessary parameters consist of kinetical properties of the assimilation process and other physiological parameters (which have to be taken from extant plants), as well as physical constants and anatomical parameters which can be obtained from well-preserved fossil specimens. The model system is applied to an Early Devonian land plant, *Aglaophyton major*. The results demonstrate that, under an Early Devonian CO_2 concentration, *A. major* shows an extremely low transpiration rate and a low, but probably sufficiently high assimilation rate. Variation of the atmospheric CO_2 concentration shows that the assimilation is fully saturated even if the CO_2 content is decreased to about one-third of the initial value. This result indicates that *A. major* was probably able to exist under a wide range of atmospheric CO_2 concentrations. Further applications of this model system to ecophysiological studies of early land plant evolution are discussed.

1. Introduction

Early land plants with a "rhyniophytic" habit represent the evolutive starting point of the extant terrestrial tracheophyte flora (Bateman *et al.*, 1998). As documented by the fossil record, they existed through the Silurian and Lower Devonian (about 420–380 million years ago). They are characterized by radially symmetric axes which are equipped with a central conducting bundle and which branch dichotomously (this axis type is termed telome, after Zimmermann, 1959). True roots are absent. The members of this constructionally primitive group with still unsolved systematic interrelationships (Kenrick & Crane, 1997), such as *Rhynia gwynne-vaughanii* or *Aglaophyton major*, existed in an atmosphere with a CO_2 concentration which was much higher than today (Berner, 1997). New data about the ecophysiological features of these plants not only improve our knowledge of land plant evolution and ancient ecosystems but more information concerning physiological behaviour of plants under high CO_2 concentrations is also valuable

†Author to whom correspondence should be addressed.

0022–5193/00/170091 + 17 $35.00/0

considering the current increase of carbon dioxide concentration in the atmosphere.

A more detailed knowledge about the gaseous exchange (i.e. transpiration and assimilation) of these plants is thus of increasing interest (Raven, 1994). For example, Raven (1977, 1993) estimated possible assimilation and transpiration rates of rhyniophytic plant axes. Beerling & Woodward (1997) calculated gaseous exchange of numerous fossil plants by treating the gas fluxes with the common approach of resistance models (analogous to electrical circuits, see, for example, Nobel, 1991).

In the present contribution, an approach which allows for the detailed simulation of the gas fluxes of rhyniophytic plants is introduced. With *A. major* serving as an example, we show how the local tracking of gas fluxes along the different tissues of the plant axis can be deduced from (i) assumptions based on the mechanism of diffusion and physical constants that have obviously not changed since Devonian times, (ii) anatomical and morphological properties of the plant available from well-preserved fossil remains, and (iii) assumptions concerning the mechanism of photosynthesis and the CO_2 conductance within the cells of the assimilation tissue. The kinetic properties of the assimilation process may have changed over the course of time. However, a radical difference between the kinetic properties of the key enzymes of extant C_3 plants and Devonian plants appears to be unlikely (Robinson, 1994). Thus, we may be confident that the characteristic amplitudes of assimilation parameters of extant C_3 plants overlap with those of Lower Devonian plants.

The approach presented in this article is in two respects superior to the widely used concept of describing molecular fluxes in analogy to the networks of electric currents: the latter method breaks down if (i) the molecular pathway shows axial or more complicated symmetry, and if (ii) mechanisms like carbon assimilation extract molecules from the CO_2 flux along its path.

The paper is organized as follows: first, we sketch the morphology of *A. major*, a typical rhyniophytic plant, that will serve as an example throughout the paper. Then we give a short discussion of the physics behind diffusion and indicate how the mathematical complexity of the resulting differential equation can be reduced by exploiting symmetries and approximations. Subsequently, we describe the assimilation model which will be used and the mathematical proceeding. Then the model is applied to the tissue organization of *A. major*. Finally, we give results and discuss the possible applications of the method.

2. Characteristics of *A. major*

The axes of *A. major* were approximately 20 cm high with a radius of about 2–2.5 mm (Edwards, 1986). The one-layered epidermis covered by a cuticle and equipped with a stomata is followed by an approximately two- to three-layered hypodermis. A narrow channel formed by the hypodermal cells is located directly under the stomatal pore. It should be noted that not all Lower Devonian species known so far show such a channel. The channel terminates in a small substomatal chamber leading to the system of intercellular air spaces. This system is extensive in the outer cortex which is approximately two to four cell layers thick.

The inner cortex extends to the central vascular bundle. The intercellular air spaces decrease considerably in size towards the axis centre. The spatial structure of the intercellular air spaces and anatomical details of the cells of the subhypodermal layer provide evidence that the assimilating cortex cells are located subhypodermally occupying the most peripheral region of the outer cortex (Edwards *et al.*, 1998). Thus, assimilation took place in the peripheral regions of the plant axis. For a more detailed description of the anatomy of early Devonian plants in general see, for example, Remy & Hass (1996), or Edwards *et al.* (1998).

A reconstruction of the gaseous exchange may be based on an axially symmetric slice of the axis system including all tissues from the assimilating sites outwards (see Fig. 1; note that the radial dimensions of the different layers considered in the figure do not represent the real thickness values of the tissues). The mathematical model describing the fluxes together with their generating mechanisms and its application to this geometry will be explained in the next sections.

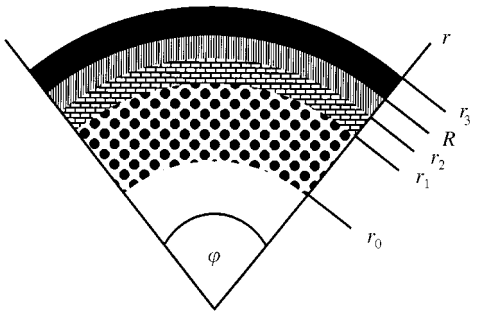

FIG. 1. A sector from the axis slice which represents the tissue model of *Aglaophyton major*. The mathematical model is applied to this system of tissue layers. Only the tissue layers which are considered by the mathematical model are shown. The other tissues, such as inner cortex or conducting tissues are not included. The z-axis is orientated perpendicularly to the illustration and thus not shown. Note that the radial dimensions of each layer as they are shown in the illustration do not reflect the real thickness values. Table 1 gives typical thickness values for each tissue layer. Boundary layer, (■); Stomatal layer, (▥); hypodermal layer, (▤); assimilation layer (▦).

3. The Model

3.1. THE PROCESS OF DIFFUSION

The movement of water vapour and CO_2 in plants is governed by the process of diffusion, i.e. Fick's first law

$$\mathbf{j} = -S \operatorname{grad} C \tag{1}$$

($[\mathbf{j}] = \mathrm{mol\,m^{-2}\,s^{-1}}$, $[S] = \mathrm{m^2\,s^{-1}}$, $[C] = \mathrm{mol\,m^{-3}}$) which states that the current density $\mathbf{j}$ (number of molecules diffusing in unit time through unit area) should be proportional to (i) the concentration gradient and (ii) an effective conductance S which depends on the properties of the diffusing molecules and on the medium through which they propagate.

If CO_2 or water vapour diffuse through free air (in contrast to the network of air-filled voids between the plant cells) diffusion is not hindered by any spatial restrictions and eqn (1) reads as $\mathbf{j} = -D \operatorname{grad} C$, i.e. the effective conductance S equals the diffusion constant in free air, D ($D_{CO_2} = 1.51 \times 10^{-5}\,\mathrm{m^2\,s^{-1}}$, $D_{H_2O} = 2.42 \times 10^{-5}\,\mathrm{m^2\,s^{-1}}$). If, however, the diffusing molecules have to move along a lattice of interconnected channels, an averaging approach to this complex pathway,—the tortuosity τ—is necessary. This quantity is included into the effective conductance S in order to keep eqn (1) valid. A second correction to S—the porosity n—is imperative if eqn (1) is to be used in the framework of the porous medium approximation, which is appropriate for the simulation of the diffusion of gases in plant tissues (see Parkhurst, 1994). The porous medium approach will be discussed more in detail in a later section.

Both corrections result in

$$S = D\frac{n}{\tau^2}, \tag{2}$$

where $n := V_p/V$, with V_p being the pore volume and V the total volume of a volume element. $\tau := l_e/l$ is the tortuosity, with l_e denoting the length of the path which a molecule has to follow in order to move from one given point to another and l is the (geometrically) shortest distance between these same points.

The diffusion equation is derived by inserting Fick's first law into the principle of mass conservation. The result in polar coordinates (r, φ, z) reads as

$$S\frac{1}{r}\frac{\partial}{\partial r}\left(r\frac{\partial C}{\partial r}\right) + \frac{1}{r^2}\frac{\partial}{\partial \varphi}\left(S\frac{\partial C}{\partial \varphi}\right) + \frac{\partial}{\partial z}\left(S\frac{\partial C}{\partial z}\right)$$

$$-\frac{\partial C}{\partial t} + \frac{\partial S}{\partial r}\frac{\partial C}{\partial r} = -Q. \tag{3}$$

If the source (or sink) term $Q = Q(r, \varphi, z, t, C)$ ($[Q] = \mathrm{mol\,m^{-3}}$) is a linear function of C and if the effective conductance $S = S(r, \varphi, z)$ and appropriate boundary conditions are prescribed, the diffusion equation (3) has exactly one solution for the concentration $C = C(r, \varphi, z, t)$ of water vapour or CO_2 as a function of space and time within the whole plant or plant parts. Once $C = C(r, \varphi, z, t)$ is calculated the current density $\mathbf{j}(r, \varphi, z, t)$ follows from eqn (1).

For realistic conditions it is impossible to solve eqn (3) in all generality. In order to avoid unnecessary mathematical difficulties we use the porous medium approach (see below), assume

translatorial symmetry along the plants symmetry axis and stationary conditions. These approximations and some estimations of the possible errors caused by their application are discussed in the later section.

Aglaophyton is divided into various tissue layers (e.g. the stomatal and the hypodermal layer, see Fig. 1). Anatomical properties influencing the effective conductance S, such as porosity and tortuosity, change from one layer to the next more or less abruptly, but remain approximately constant within the individual layers. Thus, the effective conductance S is assumed to remain constant within each radial layer.

Due to these assumptions all terms but the first on the left-hand side (l.h.s.) of eqn (3) disappears and eqn (3) becomes the ordinary differential equation

$$\frac{1}{r}\frac{\mathrm{d}}{\mathrm{d}r}\left(r\frac{\mathrm{d}C}{\mathrm{d}r}\right) = -\frac{Q}{S}, \quad S = const., \quad C = C(r),$$

$$Q = Q(r, C(r)), \tag{4}$$

which will be central to our approach. Equation (1) becomes

$$j(r) = -S\frac{\mathrm{d}C(r)}{\mathrm{d}r}, \tag{5}$$

where j is defined by $\mathbf{j} = j\mathbf{e}_r$ and $\mathbf{e}_r$ is the unit vector along the r-coordinate. For each tissue layer of the axis slice, eqn (4) must be solved separately, after assigning appropriate values to S.

3.2. APPROXIMATIONS

3.2.1. *The Porous Medium Approach*

The overall structure of *Aglaophyton* consists of concentric layers which are built from smaller structures like cells and voids which obviously do not fit into the mathematically favourable picture of axial symmetry (with its sought for consequence that C and S do not depend on φ). In order to establish axial symmetry down to infinitely small structures, the porous medium approximation replaces the discontinuous arrangement of cells and voids inside the real plant by a fictitious tissue with continuous material properties which are constant in the φ direction and may vary in the r direction.

As a result of this averaging process, the permeability of a porous medium is described by two properties: (i) the porosity, which gives the percentage part of void space to the whole volume and (ii) the tortuosity. The latter quantity accounts for the fact, that a molecule cannot diffuse along a straight line but has to follow a complex network of pathways formed by the interconnected void spaces (see above). The porous medium approach was applied successfully by Parkhurst & Mott (1990) in order to study the intercellular CO_2 gradients inside the angiosperm leaves (see also the review by the Parkhurst, 1994).

3.2.2. *Stationarity*

We consider the steady state, i.e. C and S do not depend on the time ($= t$). This condition is not as restrictive as one might think: a concentration front of, say, water vapour needs a time $t \approx s^2/D_{\mathrm{H_2O}} = 0.04\,\mathrm{s}$ to diffuse a distance $s = 1\,\mathrm{mm}$ through free air. (Diffusion constant $D_{\mathrm{H_2O}} = 2.42 \times 10^{-5}\,\mathrm{m^2\,s^{-1}}$ at $T = 20^{\circ}\mathrm{C}$ and $p = 1\,\mathrm{atm}$.) The information that a change of humidity outside a plant (as caused by a sudden shower) took place needs roughly the same time to propagate it to the centre of *Aglaophyton*. Stationary conditions—on a perhaps different level—are thus re-established very quickly.

3.2.3. *Translatorial Symmetry*

As the height of *Aglaophyton* exceeds its radius by a factor of 100, we can assume that the fluxes of carbon dioxide and water vapour are oriented mainly radially, i.e. away from the plants symmetry axis. If we orientate the coordinate system in such a way that the z-axis coincides with the plant's symmetry axis, C and S do not depend on z. This is not quite true near the top and the bottom of the plant where the molecules do not move strictly radially. To estimate the error caused by ignoring this fact we assume that the flux through a given area of the plant's surface is

proportional to this area:

$$\text{error} \approx \frac{\text{flux through tips}}{\text{total flux}} \approx \frac{\text{area of tips}}{\text{total area}}$$

$$= \frac{2\pi R^2}{2\pi R^2 + 2\pi R h} = \frac{R}{R+h} \approx \frac{R}{h} - \left(\frac{R}{h}\right)^2, \quad (6)$$

where we have used $R \ll h$. Typical values for *Aglaophyton* are $h \approx 20\,\text{cm}$ and $R \approx 2\,\text{mm}$, implying an error of about 1%.

3.3. PHOTOSYNTHESIS

Before solving eqn (4) for the assimilation layer we must specify the model of photosynthesis which will be applied, and connect it to eqn (4). We employ the photosynthetic models of Harley & Sharkey (1991) and Kirschbaum & Farquhar (1984) (both based on an older model of Farquhar *et al.*, 1980) to construct an explicit expression for the CO_2 sink $Q = Q(C)$ generated by assimilation. The core of the model consists of the equation

$$A^{chl}(q) = \left(1 - \frac{p_o}{2\tau\, q}\right) \min\{W_c(q), W_j(q)\}, \quad (7)$$

where

$$W_c(q) := \frac{q\, V_{max}}{q + K_c(1 + p_o/K_o)},$$

$$W_j(q) := \frac{q\, J}{4(q + p_o/\tau)},$$

$$J := \frac{\alpha I}{\sqrt{1 + (\alpha I/J_{max})^2}}$$

and $\min\{W_c(q), W_j(q)\}$ denotes the smaller of $W_c(q)$ and $W_j(q)$ for a given q. The carboxylation rate is limited by the activity of Rubisco ($W_c(q)$) or by the regeneration of Rubisco via electron transport ($W_j(q)$). Thus, this equation states that the net rate A^{chl} ($[A^{chl}] = \text{mol}\,\text{m}^{-2}\,\text{s}^{-1}$) of CO_2 flowing into (or out of) the chloroplasts depends on the partial pressure q ($[q] = \text{Pa}$) of CO_2 at the photosynthesizing sites inside the chloroplasts, as well as on p_o, α, τ, K_c, K_o, V_{max}, I, J and J_{max} which represent the various parameters of the photosynthesis model (Table 1). Respiration is not included in the model approach.

Equation (7) is qualitative in the sense (Parkhurst, 1994) that the functional form of $A^{chl}(q)$ is not derived from the first biochemical principles but may be chosen more or less arbitrarily as long as C_3-plant-specific features such as limitation of photosynthesis by Rubisco activity or by RuP_2 regeneration due to electron transport are maintained.

The implementation of the photosynthesis model (7) into the diffusion equation (4) requires the following tasks:

(i) $A^{chl}(q)$ is connected to Q by bookkeeping considerations which involve the porosity n_{as} (= percentage part of the volume of the assimilating tissue occupied by intercellular air spaces), the surface-to-volume ratio (a_{as}/v_{as}) of a typical cortex cell, and the ratio (a_{chl}/a_{as}) of the sum of the surfaces of all chloroplasts a_{chl} within one cortex cell to the surface a_{as} of this cell. These parameters have to be considered, because photosynthesis takes place in the chloroplast layer located peripherally of an assimilating cell. The CO_2 pathway thus includes the crossing of cell walls and cell membranes, a short distance in the cytosol and crossing of the chloroplast limiting membranes (see Nobel, 1991). The corresponding surface areas of these components have to be taken into account.

The result is

$$Q = -\left(\frac{a_{chl}}{a_{as}}\right)\left(\frac{a_{as}}{v_{as}}\right)(1 - n_{as})\, A^{chl}(q). \quad (8)$$

(ii) The partial pressure q of CO_2 inside the chloroplasts in eqn (7) should be replaced by the CO_2 concentration $C(r)$ in the intercellular air spaces of the assimilation layer. Following Parkhurst & Mott (1990) and Parkhurst (1994), we use

$$A^{chl} = g_{liq}(C(r)\, R_{gas}\, T - q), \quad (9)$$

TABLE 1
Aglaophyton *specific parameters*

Parameter	Value units	Abbreviation
Boundary values		
$C_{atm}^{CO_2}$	168 mmol m^{-3}	Atmospheric carbon dioxide concentration
$C_{atm}^{H_2O}$	480 mmol m^{-3}	Atmospheric water vapour concentration
$C_{sat}^{H_2O}$	960.3 mmol m^{-3}	Saturation value of water vapour at 20°C and 1 atm
V_l^m	1.805×10^{-8} m^3 $mmol^{-1}$	Molar volume of water at 20°C
γ	0.0728 Pa m	Surface tension of water at 20°C
Boundary layer		
r_3	2.685×10^{-3} m	Outer edge of the boundary layer
d_{bl}	0.435×10^{-3} m	Thickness of the boundary layer
v_{atm}	0.8 m s^{-1}	Atmospheric wind velocity
n_{bl}	1 —	Porosity of the boundary layer
τ_{bl}	1 —	Tortuosity of the boundary layer
Stomatal layer		
R	2.25×10^{-3} m	Radius of the plant
d_{st}	0.03×10^{-3} m	Depth of the stomatal pore
a_{st}	3.22×10^{-10} m^2	Surface area of the stomatal pore
v_{st}	1.0×10^6 m^{-2}	Number density of the stomata
n_{st}	0.32×10^{-3} —	Porosity of the stomatal layer
τ_{st}	1.34 —	Tortuosity of the stomatal layer
Hypodermal layer		
r_2	2.22×10^{-3} m	Outer edge of the hypodermal layer
d_{hy}	0.075×10^{-3} m	Thickness of the hypodermal layer
h_{hy}	0.04×10^{-3} m	Long axis of the cross-section of the hypodermal channel
w_{hy}	0.03×10^{-3} m	Short axis of cross-section of the hypodermal channel
n_{hy}	0.96×10^{-3} —	Porosity of the hypodermal layer
τ_{hy}	1 —	Tortuosity of the hypodermal layer
Assimilation layer		
r_1	2.145×10^{-3} m	Outer edge of the assimilation layer
d_{as}	0.25×10^{-3} m	Thickness of the assimilation layer
r_0	1.895×10^{-3} m	Inner edge of the assimilation layer
σ	55×10^{-6} m	Radius of a cortex cell
(a_{as}/v_{as})	36 364 m^{-1}	Specific surface of a cortex cell
(a_{chl}/a_{as})	2.345 —	Sum of surfaces of all chloroplasts within a cortex cell over surface of one cortex cell
g_{liq}	0.5×10^{-3} mmol m^{-2} s^{-1} Pa^{-1}	Liquid-phase conductance for carbon dioxide in water from cell wall to chloroplast
n_{as}	0.35 —	Porosity of the assimilation layer
τ_{as}	1.57 —	Tortuosity of the assimilation layer
Photosynthesis		
p_o	20 260 Pa	Partial pressure of oxygen at chloroplasts
τ	2822 —	Specificity factor for Rubisco
V_{max}	0.38×10^{-3} mmol m^{-2} s^{-1}	Local maximum carboxylation rate
K_c	63.6 Pa	Michaelis–Menten constant for carboxylation
K_o	34 825 Pa	Michaelis–Menten constant for oxygenation
J	—mmol m^{-2} s^{-1}	Potential rate of electron transport
J_{max}	1.02×10^{-3} mmol m^{-2} s^{-1}	Light-saturated rate of electron transport
I	0.050 mmol m^{-2} s^{-1}	Irradiance
α	0.2–	Efficiency of light conversion

which is a spatially averaged analogue to Fick's first law (1). $R_{gas} = 8.3143\,\mathrm{m^3 Pa\,mol^{-1}\,°C^{-1}}$ is the gas constant, $T = 293.15\,\mathrm{K}$ the absolute temperature in degrees Kelvin and g_{liq} ($[g_{liq}] = \mathrm{mol\,m^{-2}\,s^{-1}\,Pa^{-1}}$) denotes the effective conductance through the interior structures of the cortex cells. The value of g_{liq} must be estimated from extant plants (see Parkhurst & Mott, 1990). Equating eqns (7) and (9), solving this relation for q as a function of $C(r)$ and substituting the result back into eqn (9), would lead to an expression for A^{chl} in terms of $C(r)$, so that via eqn (8) the differential equation (4) for the CO_2 concentration in the assimilating region would be given explicitly.

The last step, however, leads to a nonlinear differential equation for $C(r)$, which cannot be solved in a closed form. In order to circumvent this problem, we make use of the freedom granted by the fact that $A^{chl}(q)$ is only of qualitative nature. That is, we replace $A^{chl}(q)$ as given by eqn (7) by a linear approximation $A^{chl}_{lin}(q)$, which retains the crucial features of eqn (7) and casts eqn (4) into an everywhere linear differential equation in C. Details of these manipulations can be found in Appendix A.

3.4. THE SOLUTION PROCEDURE

The layer specific versions of the diffusion equation (4) as they will be applied further on sum up to (bl = boundary layer, st = stomata layer, hy = hypodermal layer, as = assimilation layer)

$$\frac{\mathrm{d}^2 C_i}{\mathrm{d}r^2} + \frac{1}{r}\frac{\mathrm{d}C_i}{\mathrm{d}r} = \begin{cases} 0 & \text{if } r_1 \leqslant r \leqslant r_3 \quad (\text{i.e. } i = bl,\ st,\ hy), \\ \chi & \text{if } r_c \leqslant r \leqslant r_1 \quad (\text{i.e. } i = as), \\ k^2 C - \kappa & \text{if } r_0 \leqslant r \leqslant r_c \quad (\text{i.e. } i = as). \end{cases} \tag{10}$$

χ, k, and κ result from the application of the linear approximation to the photosynthesis model (see Appendix A for a detailed representation). r_c divides the assimilation layer into two areas, a peripheral and an inner zone. CO_2 production is allowed to take place only in the inner zone. The necessity and derivation of r_c is explained in Appendix A.

In mathematical terms, eqn (10) represents a boundary value problem. In order to solve it, we have to match layer specific solutions of eqn (10) in such a way that the overall solution $C(r)$ becomes a continuously differentiable function of r which assumes arbitrarily prescribed values for $C(r)$ (and—depending on the circumstances—perhaps $j(r)$) at the boundaries of the considered region.

General solutions of eqn (10) can be found in text books on Theoretical Physics (for example, Arfken, 1970 or Morse & Feshbach, 1953). In the case of CO_2 diffusion, they are cited in eqn (11) and for water vapour diffusion in eqn (12) [$I_n(x)$ and $K_n(x)$ denote the modified Bessel functions of, respectively, the first and second kind of order n according to the conventions of Abramowitz & Stegun (1972)]. The A_i and B_i (resp. a_i and b_i) are arbitrary constants to which definite values will be assigned during the matching procedure.

The physical basis of the continuity requirement lies in the mobility of the molecules in a gas (or a fluid), which prevents discontinuous concentrations and fluxes. Within the various layers, continuity is already guaranteed by the mathematical structure of eqn (10).

r	$C^{CO_2}(r)$	$j^{CO_2}(r)$
r_3		
Boundary layer	$A_{bl} + B_{bl} \ln\left(\frac{r}{R}\right)$	$-S_{bl} \frac{B_{bl}}{r}$
R		
Stomatal layer	$A_{st} + B_{st} \ln\left(\frac{r}{R}\right)$	$-S_{st} \frac{B_{st}}{r}$
r_2		
Hypodermal layer	$A_{hy} + B_{hy} \ln\left(\frac{r}{R}\right)$	$-S_{hy} \frac{B_{hy}}{r}$
r_1		
Intracellular air space (outer cortex)	$A_2 + B_2 \ln\left(\frac{r}{R}\right) + \frac{\chi}{4} r^2$	$-S_{as}\left[\frac{B_2}{r} + \frac{\chi}{2} r\right]$
r_c		
	$A_1 I_0(kr) + B_1 K_0(kr) + \frac{\kappa}{k^2}$	$S_{as} k[-A_1 I_1(kr) + B_1 K_1(kr)]$
r_0		

(11)

r	$C^{H_2O}(r)$	$j^{H_2O}(r)$
r_3		
Boundary layer	$a_{bl} + b_{bl} \ln\left(\frac{r}{R}\right)$	$-S_{bl} \frac{b_{bl}}{r}$
R		
Stomatal layer	$a_{st} + b_{st} \ln\left(\frac{r}{R}\right)$	$-S_{st} \frac{b_{st}}{r}$
r_2		
Hypodermal layer	$a_{hy} + b_{hy} \ln\left(\frac{r}{R}\right)$	$-S_{hy} \frac{b_{hy}}{r}$
r_1		

(12)

Critical areas, where continuity has to be ensured explicitly, are the boundaries which separate the layers. Therefore, we require at $r = r_2$: $A_{st} + B_{st}\ln(r_2/R) = A_{hy} + B_{hy}\ln(r_2/R)$ (for the concentration), and $-S_{st}B_{st}/\ r_2 = -\ S_{hy}B_{hy}/r_2$ (for the flux), and similar relations at $r = R$, r_1 and r_c. Analogous conditions apply for solutions (12) in the case of water vapour diffusion.

As boundary conditions at $r = r_0$ and $r = r_3$ we prescribe $j^{CO_2}(r_0) = 0$ and $C^{CO_2}(r_3) = C^{CO_2}_{atm}$ in the case of CO_2 ($C^{CO_2}_{atm}$ denotes the CO_2 concentration in the free atmosphere outside the boundary layer). In the case of water vapour diffusion, we assume that the inner cortex of *Aglaophyton* (which is almost free from intercellular spaces) is saturated with liquid water, that is supplied by the central vascular bundle and evaporates in the intercellular voids of the outer cortex. As the boundary condition at $r = r_1$ we require therefore $C^{H_2O}(r_1) = C^{H_2O}_{sat} \times \exp(-(2\,V^m_l\gamma)/(R_{gas}T\sigma))$ where $C^{H_2O}_{sat}$ is the saturation value of water vapour in air above a water surface. The exponential factor is supplied by the Kelvin-equation; σ denotes the radius of a typical cortex cell, V^m_l the molar volume of water and γ the surface tension in a boundary surface that separates air and liquid water. As boundary conditions at $r = r_3$ we define $C^{H_2O}_{bl}(r_3) = C^{H_2O}_{atm}$, i.e. we prescribe the water vapour concentration $C^{H_2O}_{atm}$ in the free atmosphere outside the boundary layer.

In order to calculate $C^{CO_2}(r)$ and $j^{CO_2}(r)$ explicitly, we insert the layer-specific solutions (11) into the continuity and boundary conditions. As the layer-specific solutions depend on the unknown constants A_i and B_i, a system of ten linear equations results for the ten A_i and B_i, which can be solved for the A_i and B_i by mathematical standard procedures. By this step, the A_i and B_i become functions of the parameters that describe the plants anatomy and its photosynthetical machinery. Thus, reinsertion of the A_i and B_i back into solutions (11) will complete the solution process: C^{CO_2} and j^{CO_2} depend now only on anatomical and photosynthetic parameters plus the variable r. a_i, b_i, $C^{H_2O}(r)$ and $j^{H_2O}(r)$ are calculated similarly.

The resulting expressions are very lengthy and will therefore not be presented here. Rather, the use of a computer code, such as MAPLE, is advised for all calculations.

4. Application of the Model to the Anatomy of *A. major*

So far, the model applies to every axially symmetric plant that qualifies for the approximations stated above. In the following, we will apply the model to *A. major*. For this purpose, porosity, tortuosity and other miscellaneous quantities are calculated for the various tissue layers of *A. major*.

4.1. BOUNDARY LAYER

The first barrier which has to be taken by a diffusing molecule is the boundary layer of air which envelopes the plant. If air (or a fluid) flows around an object, a velocity gradient develops due to the adhesion of the innermost air layer to the object (see, for example, Vogel, 1994). Thickness d_{bl} and the kind of the boundary layer (laminar or turbulent) influence its conductance. For the present case, we choose the approximation given in Nobel (1991) for a cylindrical body of radius R immersed in air with a (free air) wind velocity v:

$$d_{bl} = 5.8 \times 10^{-3} m \sqrt{\frac{2R}{v}\frac{1}{s}}. \qquad (13)$$

With R as the plants radius we define the outer edge of the boundary layer as

$$r_3 := R + d_{bl}. \qquad (14)$$

The thickness of the boundary layer depends on the wind velocity and increases with decreasing wind velocity. With zero wind velocity d_{bl} and r_3 become infinite. Mathematically, this is not a problem, but the application of eqn (13) makes physically no sense in the absence of wind. A thorough discussion of this point is beyond the scope of this paper. A corresponding sensitivity study, however, demonstrated that the thickness of the boundary layer has little influence on the results, because the main resistances to diffusion are offered by the various tissue layers.

As molecules move in air unhindered by any obstacles, porosity and tortuosity take the values

$$n_{bl} = 1 \quad \text{and} \quad \tau_{bl} = 1. \qquad (15, 16)$$

4.2. STOMATAL LAYER

The conductance of the stomatal layer depends on the stomatal density, the stomatal pore size and the diffusivity of the gas. We consider only the case of fully opened stomata, due to two reasons: (i) stomatal closure requires a corresponding regulation function which is not readily available for Devonian plants, and (ii) during the closing process the size of the stomatal pore may drop below a threshold value below which interactions between the diffusing molecules and the cell walls should be taken into account, that is, Fick's first law ought to be modified in this case (Jarman, 1974; Leuning, 1983).

r_2 denotes the inner edge of the stomatal layer, d_{st} the depth of stomatal pores and thus

$$r_2 := R - d_{st}. \tag{17}$$

Fossilized specimens of *Aglaophyton* provide values for the average area of stomatal pores, a_{st}, and for the number of stomata per unit surface area, v_{st}. In order to calculate the porosity we concentrate on a "slice" of length L along the symmetry axis. We approximate the stomatal layer between R and r_2 by a thin rectangular plate of thickness d_{st} and side lengths L and $\pi(R + r_2)$, where the latter is the arithmetic mean between the circumferences of the outer edge (at $r = R$) and the inner edge (at $r = r_2$) of the stomatal layer.

The volume of one stoma is $a_{st}d_{st}$, the number of stomata on the slice of length L is $v_{st}L\pi(R + r_2)$, and therefore, the pore volume V_p is given by $V_p = a_{st}d_{st}v_{st}L\pi(R + r_2)$. Because the total volume is $V = d_{st}L\pi(R + r_2)$ and $n_{st} = V_p/V$ we obtain

$$n_{st} = a_{st}v_{st}. \tag{18}$$

In the case of the stomatal layer, tortuosity results not from the obstacles inside the stomata, but from the following effect: within the boundary layer, the lines of equal concentration of water vapour or carbon dioxide are not exactly on concentric circles (with centres coinciding with the plant's symmetry axis) but bulge out over the stomata, so that molecules diffusing out of the stomata still experience stomatal conditions although they have already left the stomatal layer in a geometric sense. Nobel (1991, p. 397) approximates this effect by an effective pore radius

$$\rho_{st} = \sqrt{\frac{a_{st}}{\pi}}. \tag{19}$$

With $l_e = d_{st} + \rho_{st}$, $l = d_{st}$ and $\tau := l_e/l$ we obtain

$$\tau_{st} = \frac{d_{st} + \rho_{st}}{d_{st}} = 1 + \frac{\rho_{st}}{d_{st}} = 1 + \sqrt{\frac{a_{st}}{\pi d_{st}^2}}. \tag{20}$$

4.3. HYPODERMAL CHANNELS

If hypodermal channels are present, their contribution to the diffusion conductance has also to be considered. We denote the thickness of the hypodermis by d_{hy} and its lower edge, the boundary to the assimilation layer, by r_1. Thus,

$$r_1 := r_2 - d_{hy} = R - (d_{hy} + d_{st}). \tag{21}$$

The derivation of porosity follows the same ideas as above. Because every hypodermal channel is attached to exactly one stoma, the number of hypodermal channels on a slice of length L equals the number of stomata, $v_{st}L\pi(R + r_2)$. As the volume of one hypodermal channel is $a_{hy}d_{hy}$ the total pore volume of all channels reads as $V_p = a_{hy}d_{hy}v_{st}L\pi(R + r_2)$. The total volume now reads as $V = d_{hy}L\pi(r_1 + r_2)$, thus,

$$n_{hy} = \frac{V_p}{V} = a_{hy}v_{st}\frac{R + r_2}{r_1 + r_2}$$

$$= a_{hy}v_{st}\frac{2R - d_{st}}{2R - (2d_{st} + d_{hy})}, \tag{22}$$

where we have used eqns (17) and (21). Hypodermal channels usually show an elliptic cross-sectional shape with the longer axis, h_{hy}, oriented parallel to the z-axis, and the shorter axis, w_{hy}, lying in a plane of $z = const$.

Thus, $a_{hy} = (\pi/4)\,h_{hy}w_{hy}$ and

$$n_{hy} = \frac{\pi}{4}h_{hy}w_{hy}v_{st}\frac{2R - d_{st}}{2R - (2d_{st} + d_{hy})}. \tag{23}$$

Hypodermal channels contain no obstacles for diffusing molecules. Their tortuosity is therefore

$$\tau_{hy} = 1. \tag{24}$$

4.4. ASSIMILATION LAYER OF THE OUTER CORTEX

The outer cortex consists of cells that look roughly like cylinders. The longitudinal axis of these cells is parallel to the longitudinal axis of the plant. Thus, in cross-sectional view, the shape of these cells is similar to circular disks. Measurements of fossil specimens yield the following average value for the porosity:

$$n_{as} \approx 0.35. \tag{25}$$

In order to calculate the tortuosity of the outer cortex, we use a rough approximation: a molecule which diffuses around such a cell has to move along a half circular path with a distance r from the cell centre. The pathlength l_e amounts to $l_e = \pi r$, the direct distance is $l = 2r$, and the following average value therefore results in

$$\tau_{as} = \frac{l_e}{l} = \frac{\pi r}{2r} = \frac{\pi}{2} \approx 1.57. \tag{26}$$

For further reference we calculate the specific surface (a_{as}/v_{as}) of an infinite-long cylindrical cortex cell with radius σ

$$\left(\frac{a_{as}}{v_{as}}\right) = \frac{2\pi\sigma}{\pi\sigma^2} = \frac{2}{\sigma}. \tag{27}$$

The thickness of the assimilation layer is denoted as d_{as} and

$$r_0 := r_1 - d_{as} = R - (d_{as} + d_{hy} + d_{st}) \tag{28}$$

represents its inner edge.

The results for the quantity $S/D = n/\tau^2$ [see eqn (2)] which apply for CO_2 as well as for water vapour are thus for the various tissue layers $(S/D)_{bl} = 1$, $(S/D)_{st} = 1.8 \times 10^{-4}$, $(S/D)_{hy} = 9.6 \times 10^{-4}$ and $(S/D)_{as} = 0.12$.

All other necessary parameters are listed in Table 1. These include (i) anatomical properties, (ii) biochemical and physiological parameters and (iii) environmental parameters. The anatomical properties are derived from thin sections of fossil *A. major* specimens. In the case of the biochemical and physiological parameters p_0, α, τ, K_c, K_0, V_{max}, I, J and J_{max} values from extant C_3 plants are applied (data compiled from Harley & Sharkey, 1991, Harley *et al.*, 1992; Wullschleger, 1993). The chosen parameters for V_{max} and J_{max} are at the lower range for modern plants (Wullschleger, 1993). The corresponding values can be found in, for example, fern leaves or conifer needles. The environmental parameters represent a Lower Devonian atmosphere as described in the literature (Berner, 1997) and an arbitrarily chosen atmospheric humidity and wind velocity.

5. Results and Discussion

Using the *Aglaophyton* specific values from Table 1 results in the plots of Fig. 2 showing the local fluxes of water vapour and CO_2 against the radial coordinate r. It is apparent that the fluxes are quite smooth functions of r outside the assimilation layer. This is to be expected from the plants axial symmetry, which forces the fluxes to vary inversely proportional to r wherever sources or sinks are absent.

The local fluxes of CO_2 and water vapour at the plant surface give the assimilation rate and the transpiration rate per plant surface area. The

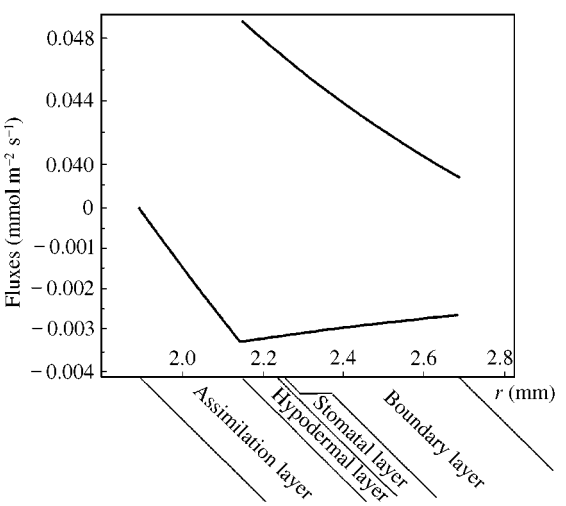

FIG. 2. Water vapour flux $j^{H_2O}(r)$ (above) and carbon dioxide flux $j^{CO_2}(r)$ (below) as a function of the radial coordinate r. $j^{CO_2}(r)$ is negative because it flows into the plant. Parameter values are as in Table 1.

value of the assimilation rate amounts to about 3.1 $\mu mol\,m^{-2}\,s^{-1}$, which is in the range of the results of Raven (1993) and Beerling & Woodward (1997). The value of the transpiration rate amounts to about 47 $\mu mol\,m^{-2}\,s^{-1}$. Both values are low, if compared to extant plants. Shade leaves of angiosperms, conifer needles or ferns show assimilation rates which lie in the range of about 6 $\mu mol\,m^{-2}\,s^{-1}$ (Larcher, 1997). The transpiration rate is extremely low, for example, as leaves of, extant herbaceous plants may reach transpiration rates of more than 5000 $\mu mol\,m^{-2}\,s^{-1}$ (Larcher, 1997). The tiny xylem strands of rhyniophytic plants thus appear to be sufficient due to the obviously low water demand of the plant axes.

The local concentrations of water vapour and CO_2 plotted in Fig. 3 against r behave less smoothly, because their gradients $dC(r)/dr = -(1/S)j(r)$ [from eqn (5)] are dominated by the factor $1/S$ which leaps considerably from layer to layer, exhibiting the proportions $1/S_{bl} : 1/S_{st} : 1/S_{hy} : 1/S_{as} \approx 1 : 5000 : 1000 : 8$. This causes steep gradients of both CO_2 and water vapour in the stomatal and hypodermal layers, whereas in the boundary layer and—in the case of CO_2—in the assimilation layer, the concentrations of both gases remain almost constant.

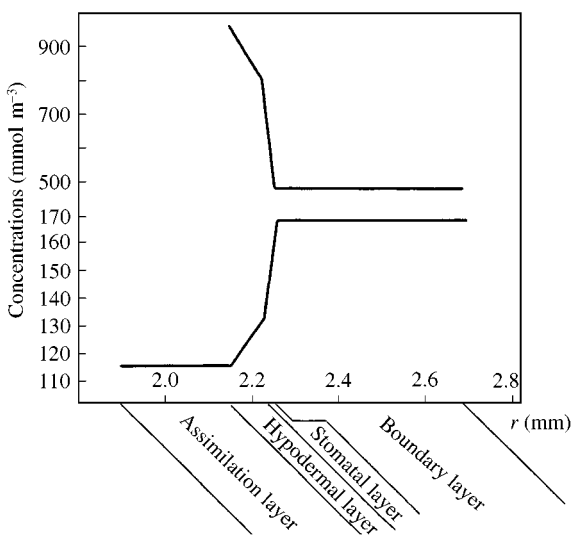

FIG. 3. Water vapour concentration $C^{H_2O}(r)$ (above) and carbon dioxide concentration $C^{CO_2}(r)$ (below) as a function of the radial coordinate r. Parameter values are as in Table 1.

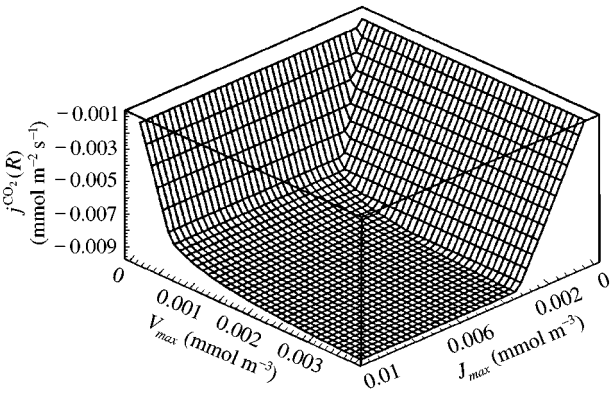

FIG. 4. Assimilation rate $j^{CO_2}(R)$ as a function of V_{max} and J_{max}. The original input values amount to $V_{max} = 0.38\ \mu mol\,m^{-2}\,s^{-1}$ and $J_{max} = 1.02\ \mu mol\,m^{-2}\,s^{-1}$. Other input values are as in Table 1.

As many input values represent estimations or are borrowed from extant plants, a number of sensitivity studies were carried out in order to yield an impression of how the results are influenced by smaller or greater changes of these input parameters. For these sensitivity studies, the calculations are repeated with one or two parameters of the whole set of input parameters increasing and decreasing systematically. Figure 4 shows the assimilation rate ($= j^{CO_2}(R)$) plotted against V_{max} and J_{max}. $j^{CO_2}(R)$ increases almost linearly with increasing V_{max} and J_{max} (with the other parameters remaining constant) up to a value of $j^{CO_2}(R)$ of about 8 $\mu mol\,m^{-2}\,s^{-1}$. At this point, V_{max} and J_{max} amount to about 0.4 and 3 $\mu mol\,m^{-2}\,s^{-1}$, respectively. Beyond this point, $j^{CO_2}(R)$ increases slowly approaching an upper limit of about 0.01 $mmol\,m^{-2}\,s^{-1}$. The values which are originally chosen for the simulations lead to a result which lies in the lower range of these possible values ($j^{CO_2}(R) = 3.1\ \mu mol\,m^{-2}\,s^{-1}$). The chosen input values of V_{max} and J_{max} are therefore located in the critical interval of possible values.

In another sensitivity study, the value of g_{liq}, the liquid-phase conductance for carbon dioxide in water (from the cell wall to the chloroplasts), was varied. The graph in Fig. 5 shows that the parameter of g_{liq} has no influence on the assimilation rate, until it reaches unrealistically low values. Note that the scale of g_{liq} ends at $5 \times 10^{-6}\ mmol\,m^{-2}\,s^{-1}\,Pa^{-1}$, a value much

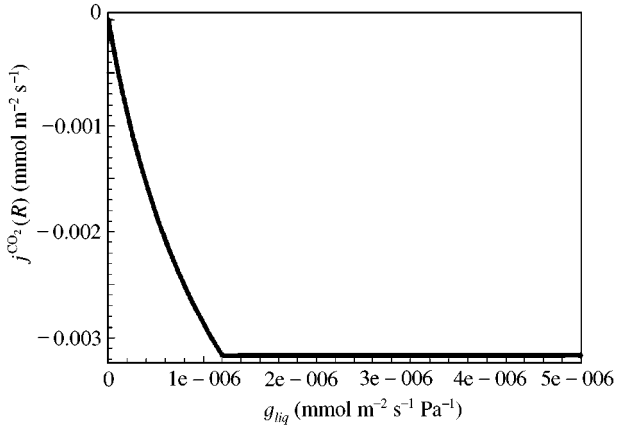

FIG. 5. Assimilation rate $j^{CO_2}(R)$ as a function of g_{liq}, the liquid-phase conductance for carbon dioxide in water. The scale of g_{liq} ends at 5×10^{-6} mmol m^{-2} s^{-1} Pa^{-1}, a value much lower than the original input value, $g_{liq} = 0.5 \times 10^{-3}$ mmol m^{-2} s^{-1} Pa^{-1}. All other parameter values are as in Table 1.

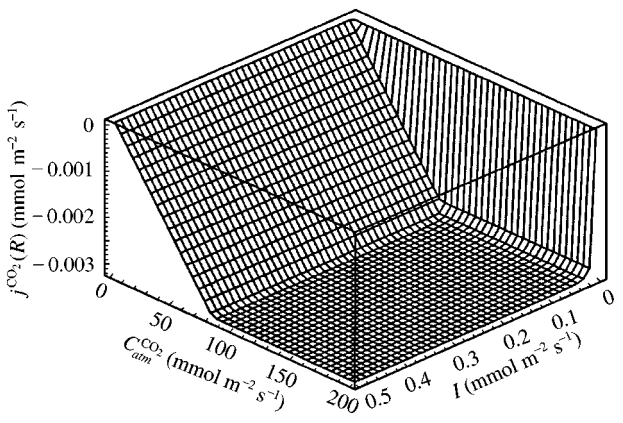

FIG. 6. Assimilation rate $j^{CO_2}(R)$ as a function of the irradiance I and the atmospheric carbon dioxide concentration $C_{atm}^{CO_2}$. The original input values amount to $I = 50$ μmol m^{-2} s^{-1} and $C_{atm}^{CO_2} = 168$ mmol m^{-2} s^{-1}. All other parameter values are as in Table 1.

lower than the chosen parameter taken from the literature.

The irradiance I was also varied (see Fig. 6). The results show that increasing I beyond the chosen input value has no influence on $j^{CO_2}(R)$. If I is decreased, however, $j^{CO_2}(R)$ decreases correspondingly. A lower irradiance value due to, for example, shading, thus decreases the assimilation rate.

These sensitivity studies demonstrate that increasing or decreasing input values may or may not have an effect on the simulation results, depending on the parameters. As many quantities must be estimated or taken from results obtained with extant plants, sensitivity studies can be used to identify critical parameters. The validity of obtained simulation results must then be checked by using additional criteria. Interestingly, the intercellular CO_2 concentration inside the assimilating tissue amounts to about 116 mmol m^{-3}, which corresponds to about 69% of the external value. Extant plants also show intercellular CO_2 concentrations which amount to 70% of the external value (von Caemmerer & Evans, 1991). The fact that the intercellular CO_2 concentration obtained by the calculations corresponds to this value thus indicates that the chosen input values represent reasonable estimations (see below).

If the water use efficiency (WUE), under stationary circumstances defined by

$$\text{WUE} := \frac{\text{number of } CO_2 \text{ molecules fixed}}{\text{number of } H_2O \text{ molecules transpired}} = \frac{|j^{CO_2}(R)|}{j^{H_2O}(R)} \tag{29}$$

is calculated, then we obtain a value of 0.068 which is 34 times higher than the typical values for extant C_3 plants (see, for example, Kramer, 1983). This high value is mainly due to the low transpiration rate of the rhyniophytic plant axis.

As stated by Edwards *et al.* (1998), the low stomatal density and the presence of the hypodermal layer should reflect a water-conserving strategy. In fact, the results demonstrate an extremely low water loss caused by the low stomatal density plus the additional resistance of the hypodermal layer. A direct comparison of rhyniophytic plants to extant plants in order to gain information about, for example, their environmental conditions is difficult and may lead to misinterpretations, because the primitive architecture of these earliest land plants is coupled to the pioneering colonization of the terrestrial environment (Edwards, 1998). As true roots were absent in rhyniophytic plants, they probably showed a low water-absorbing capacity. Mycorrhizal fungi were present in these plants. However, it is assumed that water absorption took place in the underground rhizoids of the plants.

Thus, the low water loss perhaps matched the probably low-water-absorbing capacity of these plants. Despite the low transpiration rate, the photosynthetic process reached assimilation rates which are low if compared to extant plants, but probably sufficiently high for rhyniophytic plant axes due to the high CO_2 content of the Lower Devonian atmosphere. Thus, as was stated by Edwards (1998), "it could be argued that high CO_2 concentration "permitted" the minimizing of numbers of stomata (...)".

As a high atmospheric CO_2 content probably represents a prerequisite for the evolution of early terrestrial plants such as *Aglaophyton major*, the question arises to which limit of the atmospheric CO_2 concentration rhyniophytic plants were able to exist. In order to study how the assimilation process changes with external CO_2 concentration, the latter is varied while all other parameters remain constant. Figure 6 illustrates the assimilation rate ($= CO_2$ flux into the plant surface) plotted against the atmospheric CO_2 concentration. The graph shows that the assimilation rate is roughly constant and fully saturated over a wide range of atmospheric CO_2 concentrations. Below a CO_2 concentration of about 81 mmol m^{-3} the assimilation rate decreases approximately linearly with decreasing atmospheric CO_2 content. Lower values than those which represent the upper limits or average values of the estimation range of Lower Devonian atmospheric CO_2 concentrations are thus sufficient for a saturation of the assimilation process and *Aglaophyton major* may well have been able to exist under a wide range of atmospheric CO_2 concentrations.

Because it is obviously impossible to conduct physiological measurements on fossil plants, some uncertainties exist for the present approach. This concerns mainly the biochemical parameters of photosynthesis. As noted above, assimilation parameters were chosen which lie in the lower range of extant C_3 plants. It is possible, for example, that the photosynthesis apparatus of rhyniophytic plants showed even lower parameters. It appears, however, reasonable to apply these values considering the fact that a wide range of C_3 plants such as conifers or ferns show parameters which are similar to the chosen values. This is supported by the resulting intercellular CO_2 concentration amounting to 69% of the external value. As discussed in Beerling & Woodward (1997), a corresponding ratio between internal and external CO_2 concentration is probably the common case for land plants, both past and present. This is supported by the relative constancy of $\delta^{13}C$ of terrestrially produced organic matter over the last 350 million years (Farquhar *et al.*, 1989). Another uncertainty is represented by such parameters as the resistance of the cell membranes to CO_2 or chloroplast content of the assimilating cells. However, the same ideas as above are valid for these parameters and it appears to be reasonable to choose the values of extant C_3 plants.

Another problem may be represented by the mycorrhizal fungi present in rhyniophytic plant axes (Taylor & Taylor, 1997). Quite probably the hyphae contributed at least to the nutrient supply of the plants, as is the case for extant mycorrhizae (Harley & Smith, 1983). Relevant to the present approach are possible influences on the following parameters: the volume (resp. porosity n_{as}) of the intercellular air spaces by simply occupying space and the permeability of the plant for external gases or fluids. The significance of the first effect may be investigated by carrying out sensitivity studies. In the case of the second effect, reasonable estimations about this possible effect would be needed. The actual model assumes that the stomatal pores are the main pathway for CO_2 and water vapour. If detailed information about the effects of the hyphae on the permeability of the plant axis became available, these could be easily introduced into the model system.

The approach presented in this paper allows readily for studying different taxa with different anatomical properties. Additionally, sensitivity studies are possible, allowing single parameters to be varied while the other values remain constant. Examples are shown in Figs 4, 5, & 6. In this way, considered environmental, anatomical and biochemical variables can be varied systematically and independently and the effects of these variations can be studied. Thus, functional studies become feasible which allow for comparisons of different taxa and to explore possible optima of the plant constructions. It is to be expected that further applications of this approach will yield numerous results concerning

ecophysiological and functional characteristics of the earliest land plants.

REFERENCES

ABRAMOWITZ, M. & STEGUN, I. (1972). *Handbook of Mathematical Functions*. New York: Dover Publications.

ARFKEN, G. (1970). *Mathematical Methods for Physicists*. New York: Academic Press.

BATEMAN, R. M., CRANE, P. R., DIMICHELE, W. A., KENRICK, P. R., ROWE, N. P., SPECK, T. & STEIN, W. (1998). Early evolution of land plants: phylogeny, physiology, and ecology of the primary terrestrial radiation. *Ann. Rev. Ecol. Systematics* **29,** 263–292.

BEERLING, D. J. & WOODWARD, F. L. S. (1997). Changes in land plant function over the Phanerozoic: reconstructions based on the fossil record. *Bot. J. Linn. Soc.* **124,** 137–153.

BERNER, R. A. (1997). The rise of plants and their effect on weathering and atmospheric CO_2. *Science* **276,** 544–545.

VON CAEMMERER, S. & EVANS, J. R. (1991). Determination of the average partial pressure of CO_2 in chloroplasts from leaves of several C_3 plants. *Austr. J. Plant Physiol.* **18,** 287–306.

EDWARDS, D. S. (1986). *Aglaophyton major*, a non-vascular land plant from the Devonian Rhynie Chert. *Bot. J. Linn. Soc.* **93,** 173–204.

EDWARDS, D. (1998). Climate signals in Paleozoic land plants. *Philos. Trans. R. Soc. Lond., Ser.* **B 353,** 141–157.

EDWARDS, D., KERP, H. & HASS, H. (1998). Stomata in early land plants: an anatomical and ecophysiological approach. *J. Exp. Bot.* **49,** 255–278.

FARQUHAR, G. D., VON CAEMMERER, S. & BERRY, J. A. (1980). A biochemical model of photosynthetic CO_2 assimilation in leaves of C_3 species. *Planta* **149,** 78–90.

FARQUHAR, G. D., EHLERINGER, J. R. & HUBICK, K. T. (1989). Carbon isotope discrimination and photosynthesis. *Ann. Rev. Plant Physiol. Plant Mol. Biol.* **40,** 503–537.

HARLEY, J. L. & SMITH, S. S. (1983). *Mycorrhizal Symbiosis*. New York: Academic Press.

HARLEY, P. C. & SHARKEY, T. D. (1991). An improved model of C_3 photosynthesis at high CO_2: reversed O_2 sensitivity explained the lack of glycerate re-entry into the chloroplast. *Photosynth. Res.* **27,** 169–178.

HARLEY, P. C., THOMAS, R. B., REYNOLDS, J. F. & STRAIN, B. R. (1992). Modelling the photosynthesis of cotton grown in elevated CO_2. *Plant, Cell Environ.* **15,** 271–282.

JARMAN, P. D. (1974). The diffusion of carbon dioxide and water vapour through stomata. *J. Exp. Bot.* **25,** 927–936.

KENRICK, P. & CRANE, P. R. (1997). The origin and early evolution of plants on land. *Nature* **389,** 33–39.

KIRSCHBAUM, M. U. F. & FARQUHAR, G. D. (1984). Temperature dependance of whole leaf photosynthesis in Eucalyptus pauciflora Sieb. ex Spreng. *Aust. J. Plant Physiol.* **11,** 519–538.

KRAMER, P. J. (1983). *Water Relations of Plants*, New York: Academic Press.

LARCHER, W. (1997). *Physiological Plant Ecology*, 3rd Edn. New York: Springer-Verlag.

LEUNING, R. (1983). Transport of gases into leaves. *Plant, Cell Environment* **6,** 181–194.

MORSE, P. M. & FESHBACH, H. (1953). *Methods of Theoretical Physics*. New York: McGraw-Hill Book Company.

NOBEL, P. S. (1991). *Physicochemical and Environmental Plant Physiology*. San Diego: Academic Press.

PARKHURST, D. F. (1994). Diffusion of CO_2 and other gases inside leaves. *Phytology* **126,** 449–479.

PARKHURST, D. F. & MOTT, K. A. (1990). Intercellular diffusion limits to CO_2 uptake in leaves. *Plant Physiol.* **94,** 1024–1032.

RAVEN, J. A. (1977). The evolution of vascular land plants in relation to supracellular transport processes. *Adv. Bot. Res.* **5,** 153–219.

RAVEN, J. A. (1993). The evolution of vascular plants in relation to quantitative functioning of dead water-conducting cells and stomata. *Biol. Rev.* **68,** 337–363.

RAVEN, J. A. (1994). The significance of the distance from photosynthesizing cells to vascular tissue in extant and early vascular plants. *Bot. J. Scotland* **47,** 65–81.

REMY, W. & HASS, H. (1996). New information on gametophytes and sporophytes of Aglaophyton major and inferences about possible environmental adaptations. *Rev. Palaeobot. Palynol.* **90,** 175–193.

ROBINSON, J. M. (1994). Speculations on carbon dioxide starvation, Late Tertiary evolution of stomatal regulation and floristic modernization. *Plant, Cell Environ.* **17,** 345–354.

TAYLOR, T. N. & TAYLOR, E. L. (1997). The distribution and interactions of some Paleozoic fungi. *Rev. Palaeobot. Palynol.* **95,** 83–94.

VOGEL, S. (1994). *Life in Moving Fluids*. Princeton: Princeton University Press.

WULLSCHLEGER, S. D. (1993). Biochemical limitations to carbon assimilation in C_3 plants—a retrospective analysis of the A/C_i curves from 109 species. *J. Exp. Bot.* **14,** 907–920.

ZIMMERMANN, W. (1959). *Die Phylogenie der Pflanzen*. Stuttgart: Fischer.

APPENDIX A

Linear Approximation of the Photosynthesis Model

As stated in the article, the nonlinearized version of the photosynthetic model consists of the equations

$$A^{chl}(q) = \left(1 - \frac{p_0}{2\tau q}\right) \min\{W_c(q), W_j(q)\}, \quad \text{(A.1)}$$

where

$$W_c(q) := \frac{q\, V_{max}}{q + K_c(1 + p_o/K_o)},$$

$$W_j(q) := \frac{q\, J}{4(q + p_o/\tau)},$$

$$J := \frac{\alpha I}{\sqrt{1 + (\alpha I/J_{max})^2}}$$

and $\min\{W_c(q), W_j(q)\}$ denotes the smaller of $W_c(q)$ and $W_j(q)$ for a given q.

We define the linear approximation $A^{chl}_{lin}(q)$ to eqn (A.1) by (i) the straight line through the points $(q, A^{chl}) = (0, A^{chl}(0))$ and $(q, A^{chl}) = (p_o/(2\tau), 0)$ and (ii) the straight line parallel to the q-axis with the asymptotic value $A^{chl} = \min\{V_{max}, J/4\}$. q_c denotes the q value of the intersection of (i) and (ii):

$$A^{chl}_{lin}(q) := \begin{cases} V_{max} & \begin{cases} \text{if } q_s \leqslant 0 \quad \text{and } J/4 > V_{max} \quad \text{and } q_c < q, \\ \text{if } q_s > 0 \quad \text{and } J/4 > V_{max} \quad \text{and } q_c < q, \end{cases} \\ \dfrac{J}{4} & \begin{cases} \text{if } q_s \leqslant 0 \quad \text{and } J/4 < V_{max} \quad \text{and } q_c < q, \\ \text{if } q_s > 0 \quad \text{and } J/4 < V_{max} \quad \text{and } q_c < q, \end{cases} \\ \dfrac{J(2\tau q - p_o)}{8p_o} & \begin{cases} \text{if } q_s \leqslant 0 \quad \text{and } J/4 < V_{max} \quad \text{and } 0 \leqslant q \leqslant q_c, \\ \text{if } q_s > 0 \quad \text{and } J/4 > V_{max} \quad \text{and } 0 \leqslant q \leqslant q_c, \end{cases} \\ \dfrac{K_o V_{max}(2\tau q - p_o)}{2\tau K_c(K_o + p_o)} & \begin{cases} \text{if } q_s \leqslant 0 \quad \text{and } J/4 > V_{max} \quad \text{and } 0 \leqslant q \leqslant q_c, \\ \text{if } q_s > 0 \quad \text{and } J/4 < V_{max} \quad \text{and } 0 \leqslant q \leqslant q_c, \end{cases} \end{cases} \tag{A.2}$$

with

$$q_c := \begin{cases} \dfrac{(J + 8V_{max})p_o}{2\tau J} & \text{if } q_s > 0 \quad \text{and } J/4 > V_{max}, \\ \dfrac{\tau K_c J(K_o + p_o) + 2V_{max} K_o p_o}{4V_{max}\tau K_o} & \text{if } q_s > 0 \quad \text{and } J/4 < V_{max}, \\ \dfrac{2\tau K_c(K_o + p_o) + K_o p_o}{2\tau K_o} & \text{if } q_s \leqslant 0 \quad \text{and } J/4 > V_{max}, \\ \dfrac{3\,p_o}{2\,\tau} & \text{if } q_s \leqslant 0 \quad \text{and } J/4 < V_{max}, \end{cases} \tag{A.3}$$

where

$$q_s := \frac{\tau K_c J(K_o + p_o) - 4V_{max} K_o p_o}{\tau K_o(4V_{max} - J)}. \tag{A.4}$$

Equating eqn (A.2) with

$$A^{chl} = g_{liq}(C\,R_{gas}\,T - q) \tag{A.5}$$

solving for q as a function of C and substituting back into eqn (A.2) we obtain an expression for $A^{chl}_{lin}(C)$. Inserting this result into

$$Q = -\left(\frac{a_{chl}}{a_{as}}\right)\left(\frac{a_{as}}{v_{as}}\right)(1 - n_{as})\,A^{chl}(q) \tag{A.6}$$

the diffusion equation (4) attains the following form in the assimilation layer:

$$\frac{\mathrm{d}^2 C}{\mathrm{d}r^2} + \frac{1}{r}\frac{\mathrm{d}C}{\mathrm{d}r} = \begin{cases} \chi & \text{if } r_c \leqslant r \leqslant r_1, \\ k^2\,C - \kappa & \text{if } r_0 \leqslant r \leqslant r_c. \end{cases} \tag{A.7}$$

χ, κ and k are defined by

$$\chi := \frac{1}{D_{CO_2}} \times \tau_{as}^2 \left(\frac{a_{chl}}{a_{as}}\right)\left(\frac{a_{as}}{v_{as}}\right)\frac{1-n_{as}}{n_{as}} \times \begin{cases} V_{max} & \text{if } J/4 > V_{max}, \\ \dfrac{J}{4} & \text{if } J/4 < V_{max}, \end{cases} \tag{A.8}$$

$$\kappa := \frac{1}{D_{CO_2}} \times \tau_{as}^2 \left(\frac{a_{chl}}{a_{as}}\right)\left(\frac{a_{as}}{v_{as}}\right)\frac{1-n_{as}}{n_{as}} \times \begin{cases} \dfrac{-J g_{liq} p_o}{(8\, g_{liq} p_o + 2\tau J)} & \begin{cases} \text{if } q_s \leqslant 0 \quad \text{and } J/4 < V_{max}, \\ \text{if } q_s > 0 \quad \text{and } J/4 > V_{max}, \end{cases} \\ \dfrac{-g_{liq} V_{max} K_o p_o}{2\tau[g_{liq} K_c (K_o + p_o) + K_o V_{max}]} & \begin{cases} \text{if } q_s \leqslant 0 \quad \text{and } J/4 > V_{max}, \\ \text{if } q_s > 0 \quad \text{and } J/4 < V_{max}, \end{cases} \end{cases} \tag{A.9}$$

$$k^2 := \frac{1}{D_{CO_2}} \times \tau_{as}^2 \left(\frac{a_{chl}}{a_{as}}\right)\left(\frac{a_{as}}{v_{as}}\right)\frac{1-n_{as}}{n_{as}} \times \begin{cases} \dfrac{-J\tau g_{liq} R_{gas} T}{(4\, g_{liq} p_o + \tau J)} & \begin{cases} \text{if } q_s \leqslant 0 \quad \text{and } J/4 < V_{max}, \\ \text{if } q_s > 0 \quad \text{and } J/4 > V_{max}, \end{cases} \\ \dfrac{-g_{liq} V_{max} K_o R_{gas} T}{g_{liq} K_c (K_o + p_o) + K_o V_{max}} & \begin{cases} \text{if } q_s \leqslant 0 \quad \text{and } J/4 > V_{max}, \\ \text{if } q_s > 0 \quad \text{and } J/4 < V_{max}. \end{cases} \end{cases} \tag{A.10}$$

The parameter r_c, which has been introduced in eqn (A.7), is defined by the equation $C(r_c) = C_{q_c}$, where C_{q_c} is the equivalent of the pressure q_c in terms of concentration. It is obtained by equating eqn (A.2) with eqn (A.5), setting $q = q_c$ via eqn (A.3) and solving for C. r_c divides the assimilation area into two layers defined by $r_0 \leqslant r \leqslant r_c$ and $r_c \leqslant r \leqslant r_1$, respectively. In the outer part of the assimilation layer, photosynthesis then works in the "saturated mode" [i.e. the case $q_c \leqslant q$ in eqn (A.2)], and in the inner part of the layer in the "linear mode" [i.e. $0 \leqslant q \leqslant q_c$ in eqn (A.2)]. As $A_{lin}^{chl}(q)$ is a positive constant in the first case and can become negative (if $q < p_o/2\tau$) only in the second case, CO_2 production (due to a drop of the partial pressure q of carbon dioxide in the chloroplasts below the carbon dioxide compensation point) is allowed by the model only in the inner part of the assimilation layer. This is no real restriction, because the extreme cases $r_c = r_0$ or $r_c = r_1$ are allowed by the mathematics of the model, meaning that the complete layer assimilates either in the saturated or in the linear mode, respectively.

We note that the information contained in the right-hand side (r.h.s.) of eqn (A.7) divides into the three categories of assumptions (and reliability) [according to eqns (A.8)–(A.10)] discussed in former sections: the first factor, $1/D_{CO_2}$, is a time-independent constant of nature, the second factor contains—apart from (a_{chl}/a_{as})—measurable quantities obtained from the fossil record, and the third factor reflects photosynthetic considerations for extant C_3-plants. In contrast, the water vapour flux depends only on the first two categories and is therefore less prone to the imponderabilities of evolution.